CrossMark

The Role of Zinc Phosphate Pigment in the Anticorrosion Properties of Bisphenol A Diglycidyl Ether-Polyaminoamide Coating for Aluminum Alloy AA2024-T3

O. Dagdag[1] · A. El Harfi[1] · L. El Gana[2] · Z. Hlimi[3,4] · H. Erramli[5] · O. Hamed[6] · S. Jodeh[6]

Abstract

This study is focused on an anticorrosive formulation as a coating an aluminum alloy AA2024-T3 to withstand marine environment. The anticorrosive formulation was based on an epoxy resin bisphenol-A diglycidyl ether that is cured with polyamine polyaminoamide. The anticorrosive formulation was applied onto samples of AA 2024-T3 surface with zinc phosphate (ER-ZP) and without zinc phosphate (standard). Zinc phosphate was added to the formulation in about 5 wt%. The coated AA2024-T3 substrates were evaluated by exposing them to a salt spray test chamber for various periods of time. The anticorrosive performances of the two epoxy coatings, the standard (ER) and the one containing ZP (ER-ZP), were evaluated by electrochemical impedance spectroscopy (EIS). The surface morphology of the two coatings was characterized by a scanning electron microscopy and optical microscopy. The two coated AA2024 T3 samples were tested in a harsh environment of electrolyte solution to simulate the marine environment (3 wt% NaCl solution). The value of the impedance ($|Z|_{0.01\ Hz}$) obtained by the EIS method for the standard epoxy coating (ER) and epoxy coating containing ZP (ER-ZP) were 0.88 MΩ cm^2 and 6.92 MΩ cm^2 during the 2 h of immersion in 3 wt% NaCl, respectively. After exposure for a long period of time in salt spray test chamber (4392 h) and 2 h of immersion in 3 wt% NaCl the values were dropped to 0.27 MΩ cm^2 and 0.83 MΩ cm^2, respectively. Under these conditions, a very high impedance value was obtained for AA2024-T3 samples coated with an epoxy coating containing ZP (ER-ZP). The results showed that, the ER-ZP coating surface applied on AA2024-T3 samples exposed for 4392 h showed that, the coating is homogeneous and well adhered to aluminum alloy 2024-T3 surface. The results indicated that, ZP played a dual role, it enhanced the adhesion properties of the ER coating and the coating performance as an effective barrier.

✉ O. Dagdag
  omar.dagdag@uit.ac.ma

✉ O. Hamed
  ohamed@najah.edu

[1] Laboratory of Agroresources, Polymers and Process Engineering (LAPPE), Department of Chemistry, Faculty of Science, Ibn Tofail University, BP 133, 14000 Kenitra, Morocco

[2] Laboratory of Optoelectronics, Physical Chemistry of Materials and Environment, Department of Physics, Faculty of Science, Ibn Tofail University, BP 133, 14000 Kenitra, Morocco

[3] Laboratoire de Recherche en Science des Matériaux des Milieux et de la Modélisation, Université Hassan 1er, 25000 Khouribga, Morocco

[4] Laboratory of Metallurgical Analysis, Cetim Maroc Développement, Technopole aéronautique de Nouasser, Aéroport Mohammed V, 20000 Casablanca - Nouasser, Morocco

[5] Laboratory of Materials, Electrochemistry and Environment, Department of Chemistry, Faculty of Sciences, Ibn Tofail University, Kenitra, Morocco

[6] Department of Chemistry, An-Najah National University, P. O. Box 7, Nablus, Palestine

1 Introduction

Aluminum alloys are widely utilized in many applications in various industries such as aeronautic, aerospace, and others, especially AA2024-T3 due to its outstanding mechanical and physical properties. However, aluminum alloys is easily oxidized and corroded in the corrosive environments [1–4]. Unfortunately, the adhesive strength between thin natural oxide layer on aluminum surface and subsequent organic coating is relatively poor, resulting in the insufficient protection from long-term exposure to marine environment [5].

Traditionally, the anti-corrosion properties are achieved by anodizing in chromic acid followed by organic coating [6]. Chromic anodizing (hexavalent chromium compounds) has mainly been utilized as an excellent corrosion protection [7]. However, health issues and the environmental impact caused be chromium compounds have limited its use have necessitated the development of anodizing electrolytes with reduced environmental impact [8, 9]. As a replacement for the chromic compounds, other acid electrolyte baths have been developed and applied such as sulfo-tartaric acid. Weak tartaric acid is added to strong sulfuric acid, this combination (sulfo-tartaric baths), limiting the oxide dissolution and offers an excellent corrosion resistance to aerospace alloys [10, 11]. Organic coatings have been widely applied as a barrier layer on the metal substrates, to protect them against corrosion [12]. Organic based coatings are widely used as anticorrosive for aluminum alloys structures in many industries such as aeronautics, automobiles, architecture, ships, and oil tanks [13–15]. Organic coatings received more attention due to their high chemical resistance and strong adhesion to the aluminum surface [16, 17]. The organic coatings act as a physical barrier between corrosive electrolyte and aluminum substrate [18]. Despite all the advantages of the organic coatings, some improvement are still needed such as for instance the life time the coating, since it is limited, after a long-term they tends to deteriorate and its performance as barrier declines. However, penetration of aggressive corrosive species into the standard epoxy coating from the defects and micro-pores and diffuses of these corrosive agents to the metal/coating system interface result in initiate the corrosion process and deteriorates the coating matrix. Using inhibitive pigments are added to the epoxy coatings such as chromate based pigments are the most well utilized pigments to anticorrosive protection formulations. However, because of the environmental rules, the use of this invaluable pigment in these anticorrosive formulations has been limited [19–22]. In this regard, zinc phosphate pigments have been added as less toxic alternative corrosion inhibitive pigment was one of the pigments that were used as a replacement for zinc chromate [23–25].

In this work, the formulation is a combination of epoxy resin diglycidyl ether of bisphenol (ER) cured with a poly-amine (polyaminoamide) and the pigment zinc phosphate was chosen for this purpose. The combination of these three materials produced an aluminum (AA2024-T3) coating that can endure aggressive marine environment. The anticorrosive protection properties of the formulation were monitored by the electrochemical impedance spectroscopy (EIS). The quantitative and qualitative data obtained from EIS were used to assess the coating performance. The coating surface was monitored using a SEM.

2 Experimental

2.1 Materials and Methods

The epoxy resin and hardener utilized in this work were from MAPAERO-Aerospace Coatings. The liquid epoxy is whitish in color and consists of diglycidyl ether of bisphenol-A (average molecular weight < 700), triglycidyl ether of trimethylolpropane, alkoxysilane, and nitroethane. The liquid hardener is green and consists of polyaminoamide and butan-2-ol. The pigment anticorrosive additive used in this work was zinc phosphate by purchased from Aldrich. Table 1 shows name and chemical structures used in the preparation of the coating materials and the physical and chemical properties of Zinc phosphate (ZP) are given in Table 2.

2.2 Preparation of AA2024-T3 Substrates

AA 2024-T3 specimens (wt.%: Cr 0.1; Ti 0.15; Zn 0.25; Fe 0.5; Si 0.5; Mn 0.3–0.9; Mg 1.2–1.8; Cu 3.8–4.9; others 0.15; Al balance) were cut into 8.5 cm × 4.4 cm with a thickness of 1.0 mm. The surface of the samples was polished mechanically using a disk polisher with a P1200 and P2000 SiC abrasive papers in order to obtain mirror surface. The polishing process was followed by degreasing with methyl ethyl ketone (MEK) degreasing to remove surface contaminations, washing with distilled water, and air drying.

2.3 Surface Treatment Process

2.3.1 Surface Preparation

The applied treatment sequence includes a first 15 min alkaline degreasing step (basic pH 9) (NaOH/KOH at 35 g/L) performed at 58 °C, rinsing (rinsing dead + rinsing recycled for 4 min) with distilled water at room temperature, then a 2 min sodium stripping step (NaOH 37–43 g/L) carried out at 32 °C also followed by several rinses with distilled water for 3 min at room temperature.

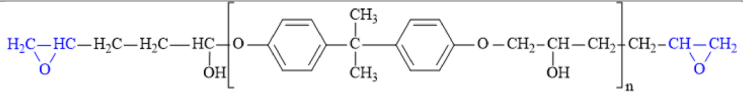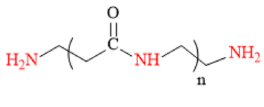**Table 1** Names and chemical structures used in the preparation of the coating materials
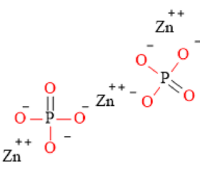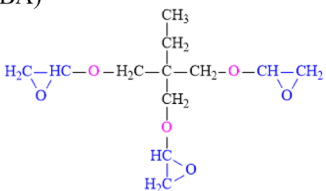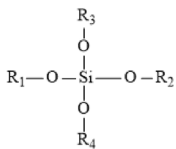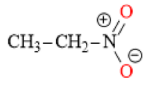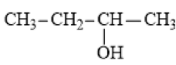
Chemical structure/ Name

Bisphenol A diglycidyl ether (DGEBA)

Polyaminoamide   Zinc phosphate (ZP)   Triglycidyl ether of trimethyl propane

Alkoxysilane   Nitroethane   Butan-2-ol

Table 2 Physical and chemical properties of Zinc phosphate (ZP)

Commercial name	Zinc phosphate ZP
Density	3.04 g/cm^3
Average particle size	4.5 μm
Oil absorption	27 cm^3/100 g
pH	7
Solubility	Insoluble in water (water: 0.03 g/L)

2.3.2 Anodizing Parameters

The anodizing process was carried out in an industrial pilot plant containing a TSA bath of 36–44 g/L of sulfuric acid (H_2SO_4) and 77–88 g/L of tartaric acid ($C_4H_6O_6$). The anodizing temperature ranges from 36 to 39 °C. The anodizing process was carried out with a potential sweep from 0 to 14 V at a rate of 2.8 V/min, followed by a plateau at 14 V for 25 min.

2.3.3 Coating Application

Two epoxy formulations were prepared and evaluated, one of them has in addition to the DGEBA epoxy resin and polyaminoamide curing agent (1:2 ratio by weight) a 5 wt% zinc phosphate (ER-ZP). In the second formulation, no zinc phosphate was used (standard coating). The two formulations were applied to AA 2024-T3 using a pneumatic suction gun. The coated samples were left at room temperature for 24 h

before post-curing at 60 °C for 1 h. The thicknesses of the dried films were about 15–25 μm.

2.4 Curing of Diglycidyl Ether of Bisphenol-A

During the curing process the epoxy resin and the curing agent polyaminoamide react to form a 3D thermoset polymer [26]. A representative scheme of the possible reaction mechanism occurs during the curing process is presented in Fig. 1. The presence of zinc ion (Zn^{2+}) during the curing stage could be an advantage, since it behaves as a Lewis acid, that coordinate to the oxygen atom of the oxirane ring, thus making the oxirane ring more susceptible for nucleophilic addition reaction with amine to undergo ring opening [27].

2.5 Evaluation of Coated Aluminum Alloy Samples

2.5.1 EIS Measurements

Electrochemical impedance spectroscopy measurements (EIS) were carried out using Potentiostat PS 200. The measurements were carried out in 3 wt% NaCl solution at room temperature. A three-electrode system was used, with the intact coating samples as the working electrode AA2024 (1 cm^2), a saturated calomel electrode (SCE) as the reference electrode and platinum as the counter electrode (CE). The EIS analysis was performed at the OCP imposed with sinusoidal amplitude of 10 mV at frequency range from 100 kHz to 10 mHz. The EIS results were fitted by EC-Lab V10.32 software. Prior to EIS measurement, the coated painted

Fig. 1 Complex formation between Zn^{2+}, epoxy resin and reaction mechanism of the polyaminoamide
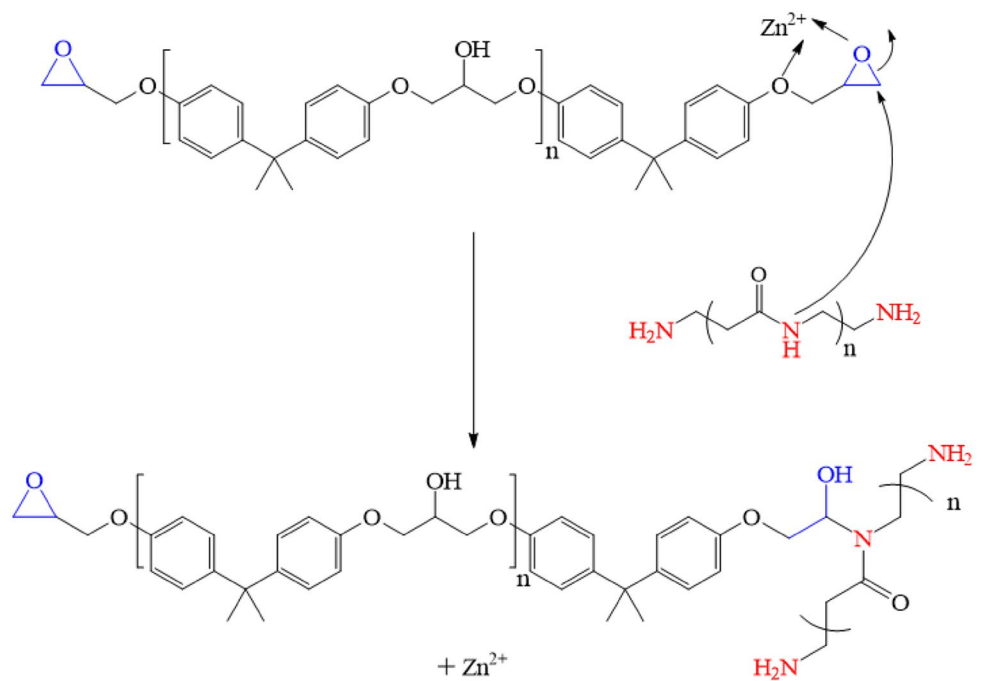
samples were immersed in the testing solution for until the OCP was stable (about 2 h).

Finally, the anti-corrosion performance of the coated panels was evaluated in accelerated environment using a salt spray test system. The corrosive nature of the chamber specified to ASTM B117 is a continuous spraying of a 5 wt% saline solution at 35 ± 2 °C.

2.5.2 Surface Characterization

The surface morphologies of two epoxy coatings (ER and ER-ZP) before and after 4392 h of exposure to salt in the spray test were analyzed by scanning electron microscopy (SEM, S3000H, Hitachi) at 20 kV. The cross-sections micrographs of coatings were evaluated by ZEISS Scope. A1 microscopy.

3 Results and Discussion

3.1 Electrochemical Impedance Spectroscopy Analysis

The EIS data analysis on coated AA2024-T3 substrates for various periods of time 1464, 2928, and 4392 h exposure and immersed for 2 h in a 3 wt% NaCl is given both as a Nyquist and as a Bode plot in Figs. 2 and 3.

In order to quantitative analysis the protective properties of the epoxy coatings ER and ER-ZP for AA2024-T3, the EIS curves were fitted with the equivalent electric circuit.

The EIS data were fitted by the equivalent circuit $R_s(Q_{coat}(R_{coat}(Q_{dl}R_{ct})))$ shown in Fig. 4.

In these circuits, R_s is the solution resistance, Q_{coat} is the constant phase element (CPE) of a coating, R_{coat} is the resistance of the electrolyte in the coating pores, Q_{dl} is the CPE of the electrical double layer, and R_{ct} is the charge transfer resistance.

The CPE was substituted for pure capacitance, due to surface heterogeneities, deviation from capacitive behavior, and dispersion effects [28].The impedance of CPE can be written as:

$$Z_{CPE} = \frac{1}{Q(j\omega)^{\alpha'}} \tag{1}$$

where Q is the CPE constant, $j = \sqrt{-1}$, ω is the angular frequency (rad/s), and α is a CPE exponent associated with the surface heterogeneity or roughness.

The electrical element parameters obtained from fitting the measured EIS data in Figs. 2 and 3 are shown Table 3.

From Figs. 2 and 3 it can be seen that, as the immersion time increases the impedance at low frequency range ($|Z|_{0.01\ Hz}$), charge transfer resistance (R_{ct}), coating resistance (R_{coat}) and decreased due to the penetration of electrolytes to the aluminum/epoxy coating interface.

At the beginning of exposure, the impedance diagrams $|Z|_{0.01\ Hz}$ of the epoxy coating ER-ZP were high and superior to 6 MΩ cm^2 during the 2 h of immersion are slightly greater than that of the standard epoxy coating ER (0.88 MΩ cm^2) in 3 wt% NaCl solution. This indicates that the epoxy coating ER-ZP provides an excellent physical
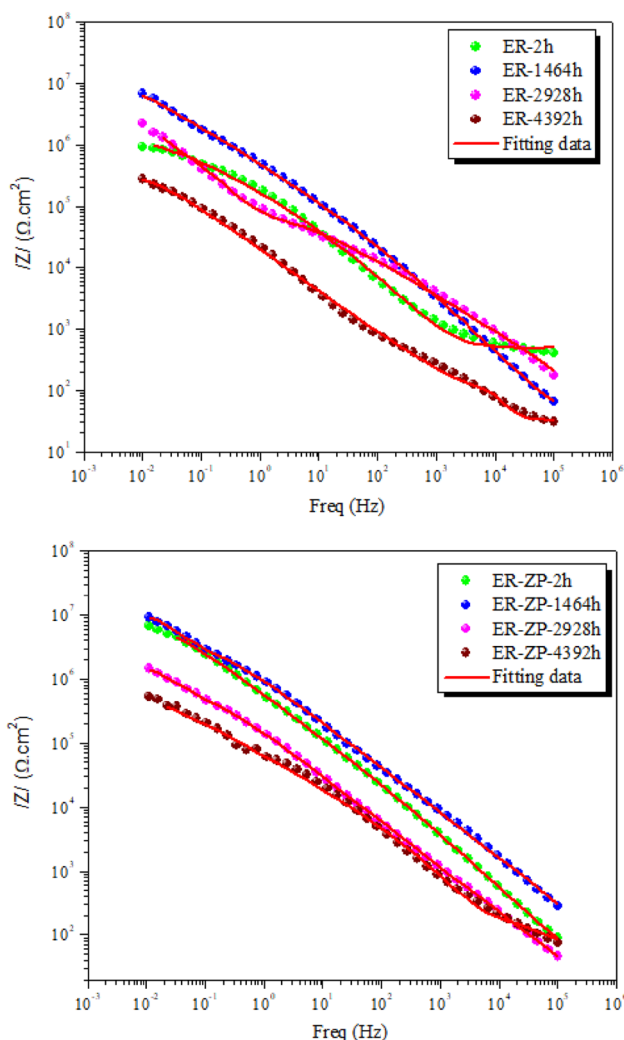
Fig. 2 Bode plots obtained for the two epoxy coatings ER and ER-ZP applied on AA2024-T3 samples for different time's exposure and 2 h of immersion in 3 wt% NaCl
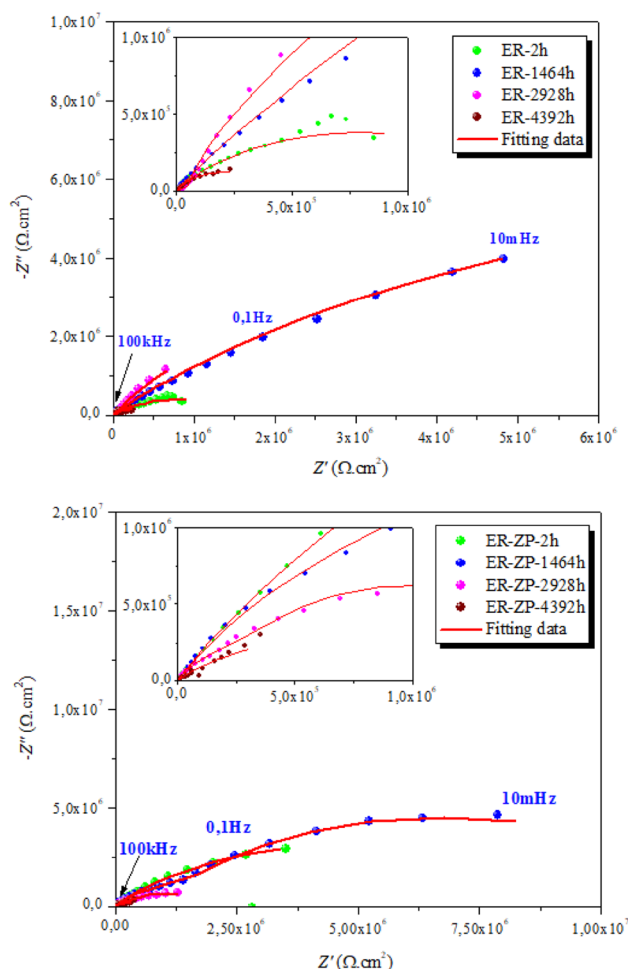

Fig. 3 Nyquist plots obtained for the two epoxy coatings ER and ER-ZP applied on AA2024-T3 samples for different time's exposure and 2 h of immersion in 3 wt% NaCl
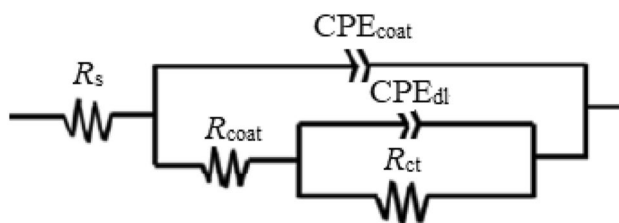
Fig. 4 The equivalent electrical circuit used to model the impedance spectra

barrier against corrosive agent's penetration though the epoxy coating matrix to AA2024-T3 surface. The impedance modulus value ($|Z|_{0.01 \text{ Hz}}$) showed an increase by increasing the exposure time from 2 to 1464 h for two the epoxy coatings ER and ER-ZP as shown in Fig. 2. The impedance modulus after 1464 h of exposure for the epoxy coating ER-ZP was greater by 9 MΩ cm² than that of the standard epoxy coating ER (2.63 MΩ cm²). This is could be an indication that, the presence of the pigment ZP beside the epoxy resin in the coating made it more stability and enhanced its anticorrosive performance. The decrease in the impedance modulus ($|Z|_{0.01 \text{ Hz}}$) values with immersion time after 1464–4392 h could be related to the diffusion of the electrolyte into the coating, thus the physical barrier properties of the film is reduced. The epoxy coating ER-ZP (0.83 MΩ cm²) is significantly higher than

the standard epoxy coating ER (0.27 MΩ cm²) in 4392 h exposure. These results confirm that the epoxy coating ER-ZP shows excellent physical barrier properties and restricted the electrolyte penetration of electrolytes to the coating/aluminum interface. As the immersion time elapsed the impedance modulus ($|Z|_{0.01 \text{ Hz}}$) decreased for two epoxy coatings ER and ER-ZP. After a long period of exposure to electrolyte, the epoxy coating deteriorated,

Table 3 The electrochemical data obtained from impedance plots of two epoxy coatings ER and ER-ZP applied on AA2024-T3 samples for different time's exposure and 2 h of immersion in 3 wt% NaCl

Sample	Time (h)	$\|Z\|_{0.01\ Hz}$ (MΩ cm^2)	R_s (Ω cm^2)	CPE$_{coat}$		R_{coat} (kΩ cm^2)	CPE$_{dl}$		R_{ct} (MΩ cm^2)	χ^2
				Q_{coat} (μF/cm^2)	α_{coat}		Q_{dl} (μF/cm^2)	α_{dl}		
ER	2	0.88	425	145	0.76	0.70	0.14	0.74	1.51	0.32
	1464	2.63	28.9	0.33	0.92	0.76	0.15	0.53	4.93	0.19
	2928	2.26	56.1	0.28	0.63	0.65	0.61	0.72	1.35	0.06
	4392	0.27	19.4	0.21	0.67	0.61	0.87	0.72	0.14	0.07
ER-ZP	2	6.92	0.37	0.21	0.66	0.24	0.04	0.95	4.35	0.27
	1464	9.23	49.4	0.56	0.70	15.0	0.12	0.93	19.2	0.21
	2928	1.61	5.01	0.84	0.71	0.30	0.26	0.84	2.00	0.17
	4392	0.83	52.6	0.83	0.71	0.15	0.28	0.93	0.44	0.32

and the penetration of electrolytes to the coating/aluminum interface and the adhesion bonds destructed. However, introduction of ZP could reduce the electrolyte penetration into the coating matrix, indicating their effect on the epoxy coating physical barrier performance enhancement [29–31].

3.1.1 Evolution of the Epoxy Coatings Protection Performance: R_{coat} and R_{ct}

The evolutions of the protection performance of two epoxy coatings ER and ER-ZP for different time's exposure can be evaluated through the coating resistance values R_{coat}. The R_{coat} indicates the ease with which the penetration of electrolytes into the epoxy coating matrix [32]. The penetration of electrolytes may filling the micro-pores and defects of epoxy coating matrix by corrosion products [33]. The decrease of R_{coat} values for different time's exposure to the diffusion of the aggressive corrosive ions into the epoxy coating matrix.

The evolution of R_{ct} values for different time's exposure is similar to that of the R_{coat} porosities. The decrease of R_{ct} values corresponds to an increase in the corrosion rate and a development of the corroded surface under the epoxy coating matrix [33].

3.1.2 Evolution of the Physical Barrier Properties: Q_{coat} and Q_{dl}

Grace to the analysis of the capacitance of epoxy coating matrix, it is possible to evaluate the adsorption of water for different time's exposure and 2 h of immersion in 3 wt% NaCl solution because the adsorption of water modifies the dielectric constant of the coating matrix, even if it is present in very small quantity. The Q_{coat} for epoxy coating (ER-ZP) is lower than standard epoxy coating (ER) during 2 h of immersion in 3 wt% NaCl solution; because ZP pigment fills the defects and micro-pores in the coating and decreases the water uptake into the coating matrix. The Q_{coat} of standard

epoxy coating ER decreases to a stable value after different time's exposure and 2 h of immersion in 3 wt% NaCl solution due to delamination of coating matrix and filling the micro-pores and defects of coating matrix by corrosion products [34]. However, the Q_{coat} for epoxy coating ER-ZP increases by increasing immersion time to 1464 h and then, a decrease in Q_{coat} value is observed after 2928 h exposure, which can be ascribed to saturation of zinc phosphate pigment structure and the decrease of hydrophilic tendency of epoxy coating ER-ZP. These results confirm that the epoxy coating ZP-ER effectively fills the micro-pores and defects. These mean that the zinc phosphate significantly enhances anticorrosive properties and the barrier role of epoxy coating matrix at long-term.

However, the Q_{dl} which is related to distribution of ionic charge at metal/coating interface [35] is significantly lower for epoxy coating ER-ZP for different time's exposure. Besides, the Q_{dl} of epoxy coating ER-ZP is lower than standard epoxy coating. The Q_{dl} value increases by extending immersion time due to expansion of active sites [36].

3.2 Salt Spray Test

The digital images of prepared two epoxy coatings (ER (a) and ER-ZP (b)) after 4392 h exposure were depicted in Fig. 5.

The standard epoxy coating ER (c) shows corroded sites on the substrate surface. For epoxy coating ER-ZP (d), less degradation is observed as compared with ER. Only small amount of white rust appears inside the scratches.

3.3 Surface Morphological of Two Epoxy Coatings

The microstructure of surfaces of two epoxy coatings (ER and ER-ZP) were characterized for change in morphology before and after 4392 h of exposure by SEM and their micrographs are shown in Fig. 6.
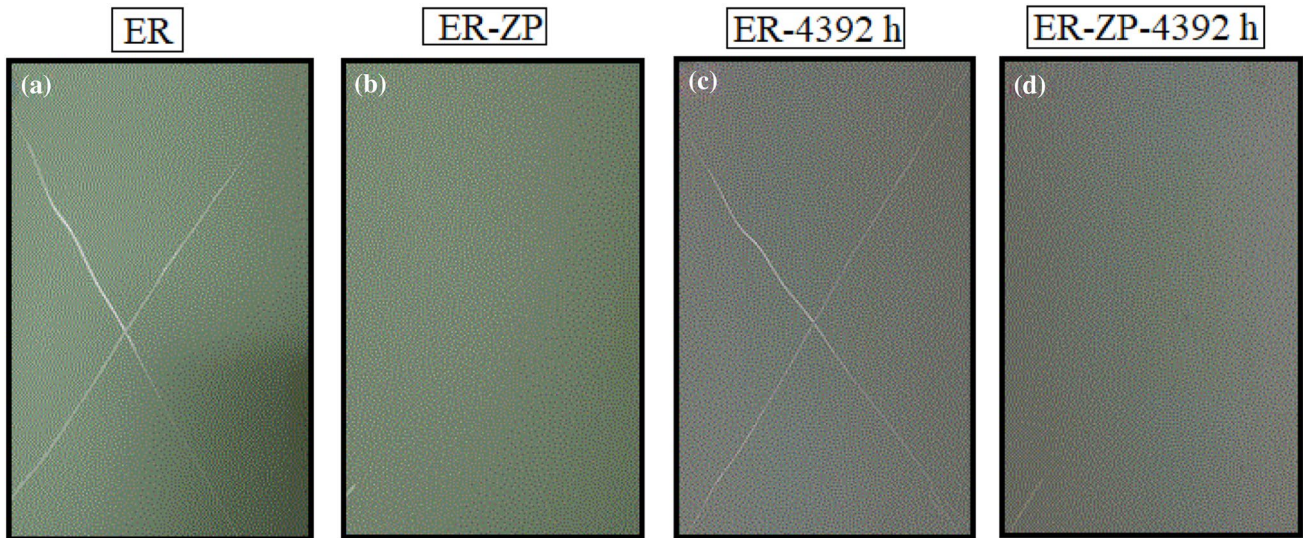
Fig. 5 Visual performance of the two epoxy coatings (ER and ER-ZP) applied on AA2024-T3 samples before and after 4392 h exposure
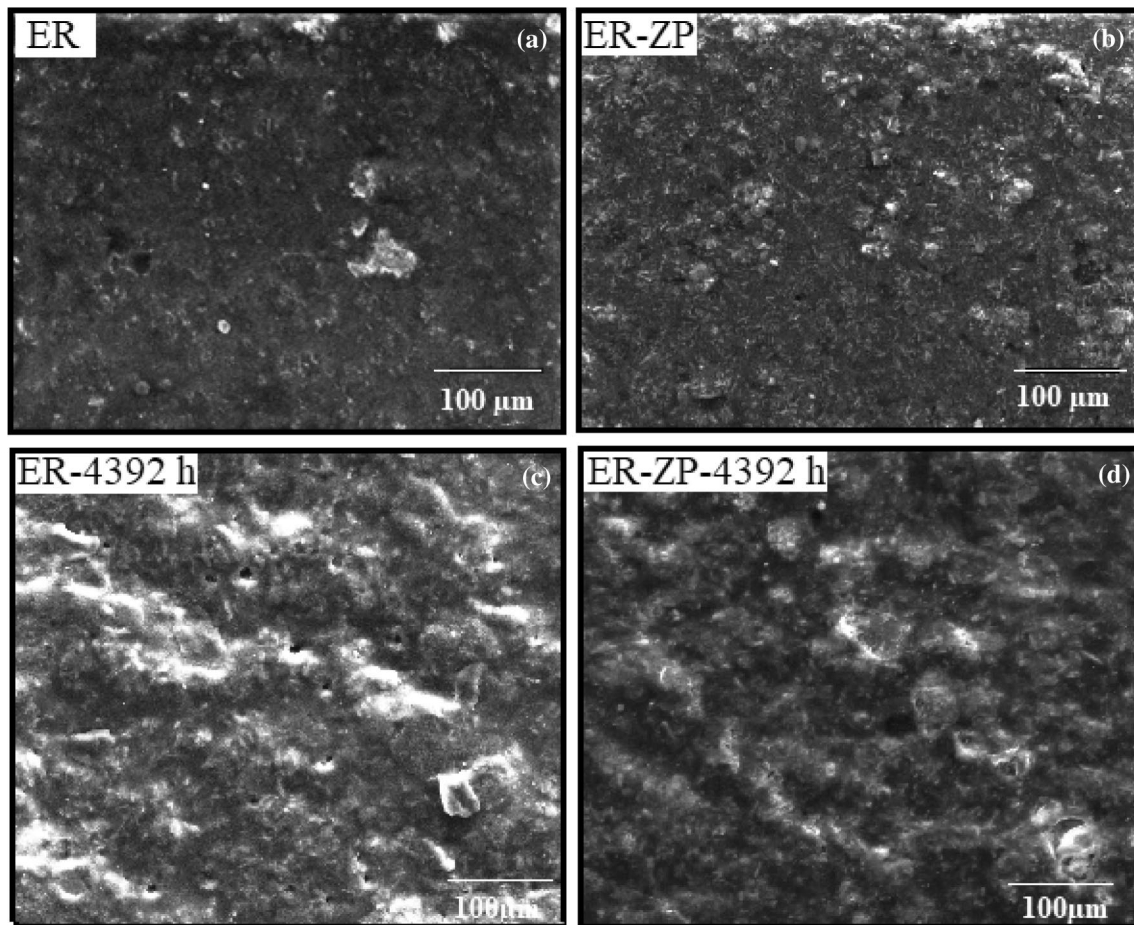

Fig. 6 SEM surface images of the two epoxy coatings (ER and ER-ZP) applied on AA 2024-T3 samples before and after 4392 h exposure

As shown in Fig. 6a, the coating defects due the structural uniformity and integrality of the coating and may degrade for the standard epoxy coating ER. On the other hand, surface the epoxy coating ER-ZP (Fig. 6b) shows a homogeneous surface and good dispersion due to the presence of ZP in this coating. This provides an excellent physical barrier that prevents the diffusion of corrosive agents though the epoxy coating matrix to AA2024-T3 surface.

The micro-pores standard epoxy coating ER surface become deep and broaden during exposure of accelerated corrosion assays as shown in Fig. 6c. The surface micropores in degraded areas significantly decreased when zinc phosphate was introduced to the epoxy coating matrix. Nevertheless, micro-pores in epoxy coating matrix were invisible after 4392 h exposure in epoxy coating ER-ZP as shown in Fig. 6d.

This provides an excellent barrier that prevents the penetration of corrosive electrolyte though the epoxy coating matrix to AA2024-T3 surface.

Figure 7 shows the surface images and a cross-section of two epoxy coatings on AA2024-T3 before and after 4392 h exposure which were investigated by optical microscope.

The full AA2024-T3 substrate was found to be homogeneously and well adhered with epoxy coating containing ZP because the AA2024-T3 metal/coating interface does not delaminate after 4392 h exposure that the standard epoxy coating after 4392 h exposure is severely damaged.

3.4 Anti-corrosion Properties of the Epoxy-ZP Matrix

The protection mechanism of the epoxy-ZP matrix is shows in Fig. 8.

As shown in Fig. 8, ZP releases the inhibitive ions such as Zn^{2+} and PO_4^{3-} at defect sites in the coating, thus forming an insoluble protective film at the anodic and cathodic sites.

The presence of Zn^{2+} at the cathodic sites assists in lowering the pH value by interacting with the hydroxyl ions, as results of that, it stabilizes the coating from undergoing cathodic delamination. Also, the formation of zinc and aluminum phosphates on the anodic sites could promote the protection of the aluminum alloy AA2024-T3 against corrosion. The higher solubility of ZP in saline solution could be another factor that promotes the formation of a more stable film on the metal surface at defect site. In addition, the ZP particle could fill the coating porosities and cavities, thus inhibiting the diffusion pathway of the electrolyte to the metal surface [37, 38].

4 Conclusions

In this study, two based epoxy coatings (ER) and (ER-ZP) were prepared and evaluated as anticorrosive for the aluminum alloy AA2024-T3.

A polymer based epoxy cured with polymeric polyamines was chosen for this study. The polymeric based epoxy has two functionality makes it unique as anticorrosive coating for AA2024-T3, it has a hydrophobic backbone and a hydrophilic end cap. Short term and long-term exposure of AA2024-T3 coated with ER-ZP showed superior performance in protecting AA2024-T3 surface against corrosion compared to the standard coating. Surface study of the coating by scanning electron microscopy (SEM) showed a homogeneous distribution of ZP in epoxy coating. The electrochemical measurements results indicate that ZP present in the coating matrix (ER-ZP) is more effective as an anticorrosive coating than the standard epoxy coating (ER). The Bode and Nyquist plots showed ER-ZP coating has outstanding barrier properties in protecting AA2024-T3 in marine environment against corrosion.
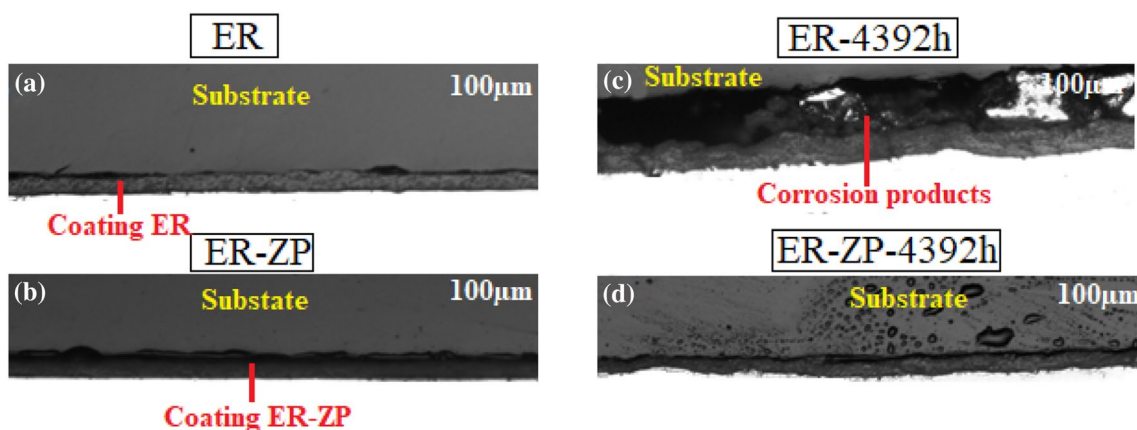

Fig. 7 Optical microscope cross-sectional morphology the two epoxy coatings (ER and ER-ZP) applied on AA 2024-T3 samples before and after 4392 h exposure
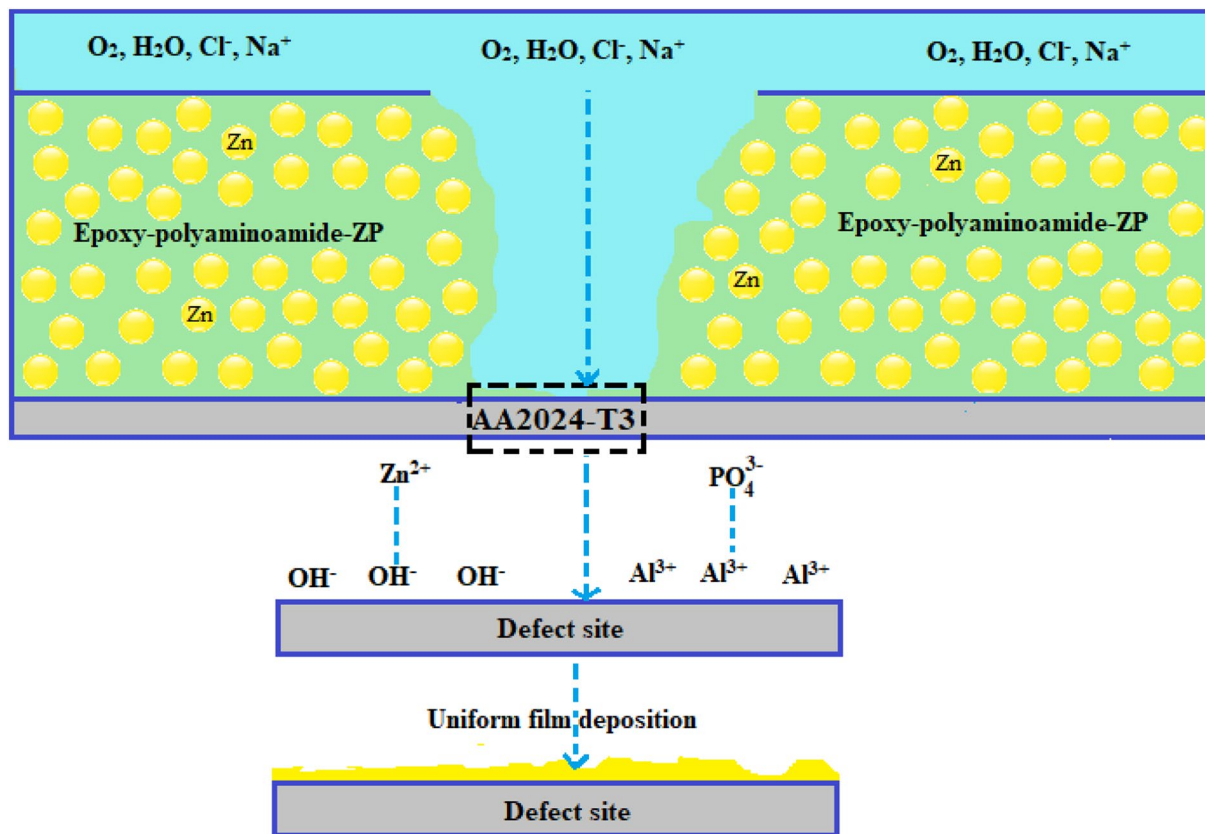
Fig. 8 Schematic mechanism of corrosion inhibition effects of ZP in the epoxy matrix

References

1. Zhu W, Li W, Mu S, Fu N, Liao Z (2017) Comparative study on Ti/Zr/V and chromate conversion treated aluminum alloys: anti-corrosion performance and epoxy coating adhesion properties. Appl Surf Sci 405:157–168
2. Dalmoro V, Alemán C, Ferreira CA, dos Santos JH, Azambuja DS, Armelin E (2015) The influence of organophosphonic acid and conducting polymer on the adhesion and protection of epoxy coating on aluminium alloy. Prog Org Coat 88:181–190
3. Mrad M, Amor YB, Dhouibi L, Montemor MF (2018) Corrosion prevention of AA2024-T3 aluminum alloy with a polyaniline/poly (γ-glycidoxypropyltrimethoxysilane) bi-layer coating: comparative study with polyaniline mono-layer feature. Surf Coat Technol 337:1–11
4. Charitha BP, Chenan A, Rao P (2017) Enhancement of surface coating characteristics of epoxy resin by dextran: an electrochemical approach. Indus Eng Chem Res 56(5):1137–1147
5. Niroumandrad S, Rostami M, Ramezanzadeh B (2016) Effects of combined surface treatments of aluminium nanoparticle on its corrosion resistance before and after inclusion into an epoxy coating. Prog Org Coat 101:486–501
6. García-Rubio M, De Lara MP, Ocón P, Diekhoff S, Beneke M, Lavía A, García I (2009) Effect of postreatment on the corrosion behaviour of tartaric–sulphuric anodic films. Electrochim Acta 54(21):4789–4800
7. Živković LS, Bajat JB, Popić JP, Jegdić BV, Stevanović S, Mišković-Stanković VB (2015) Protective properties of cataphoretic epoxy coating on aluminium alloy AA6060 modified with electrodeposited Ce-based coatings: effect of post-treatment. Prog Org Coat 79:43–52
8. Jiang MY, Wu LK, Hu JM, Zhang JQ (2015) Silane-incorporated epoxy coatings on aluminum alloy (AA2024). Part 1: improved corrosion performance. Corros Sci 92:118–126
9. Bajat JB, Milošev I, Jovanović Ž, Mišković-Stanković VB (2010) Studies on adhesion characteristics and corrosion behaviour of vinyltriethoxysilane/epoxy coating protective system on aluminium. Appl Surf Sci 256(11):3508–3517
10. Renaud A, Poorteman M, Escobar J, Dumas L, Bonnaud L, Dubois P, Olivier MG (2017) A new corrosion protection approach for aeronautical applications combining a Phenol-paraPhenyleneDiAmine benzoxazine resin applied on sulfo-tartaric anodized aluminum. Prog Org Coat 112:278–287
11. Curioni M, Skeldon P, Koroleva E, Thompson GE, Ferguson J (2009) Role of tartaric acid on the anodizing and corrosion behavior of AA 2024 T3 aluminum alloy. J Electrochem Soc 156(4):C147–C153
12. Ramezanzadeh B, Rostami M, Niroumandrad S (2017) Enhancement of the physical/mechanical properties of an epoxy composite by addition of aluminum nanoparticles through modification

with cerium oxides and functionalization by SiO_2-NH_2 thin films. Prog Org Coat 112:244–253

13. Chang CH, Huang TC, Peng CW, Yeh TC, Lu HI, Hung WI, et al (2012) Novel anticorrosion coatings prepared from polyaniline/graphene composites. Carbon 50(14):5044–5051

14. Chang KC, Ji WF, Lai MC, Hsiao YR, Hsu CH, Chuang TL, et al (2013) Synergistic effects of hydrophobicity and gas barrier properties on the anticorrosion property of PMMA nanocomposite coatings embedded with graphene nanosheets. Polym Chem 5(3):1049–1056

15. Ding J, Rahman urO, Peng W, Dou H, Yu H (2018) A novel hydroxyl epoxy phosphate monomer enhancing the anticorrosive performance of waterborne Graphene/Epoxy coatings. Appl Surf Sci 427:981–991

16. Liu S, Yan H, Fang Z, Wang H (2014) Effect of graphene nanosheets on morphology, thermal stability and flame retardancy of epoxy resin. Compos Sci Tech 90:40–47

17. Zhang Z, Zhang W, Li D, Sun Y, Wang Z, Hou C, et al (2015) Mechanical and anticorrosive properties of graphene/epoxy resin composites coating prepared by in-situ method. Inter J Mol Sci 16(1):2239–2251

18. Conradi M, Kocijan A, Kek-Merl D, Zorko M, Verpoest I (2014) Mechanical and anticorrosion properties of nanosilica-filled epoxy-resin composite coatings. Appl Surf Sci 292:432–437

19. Sanaei Z, Bahlakeh G, Ramezanzadeh B (2017) Active corrosion protection of mild steel by an epoxy ester coating reinforced with hybrid organic/inorganic green inhibitive pigment. J Alloys Compd 728:1289–1304

20. Deyab MA, Ouarsal R, Al-Sabagh AM, Lachkar M, El Bali B (2017) Enhancement of corrosion protection performance of epoxy coating by introducing new hydrogenphosphate compound. Prog Org Coat 107:37–42

21. Cotting F, Aoki IV (2016) Smart protection provided by epoxy clear coating doped with polystyrene microcapsules containing silanol and Ce (III) ions as corrosion inhibitors. Surf Coat Technol 303:310–318

22. Behzadnasab M, Mirabedini SM, Esfandeh M, Farnood RR (2017) Evaluation of corrosion performance of a self-healing epoxy-based coating containing linseed oil-filled microcapsules via electrochemical impedance spectroscopy. Prog Org Coat 105:212–224

23. Jadhav AJ, Holkar CR, Pinjari DV (2018) Anticorrosive performance of super-hydrophobic imidazole encapsulated hollow zinc phosphate nanoparticles on mild steel. Prog Org Coat 114:33–39

24. Deyab MA, De Riccardis A, Mele G (2016) Novel epoxy/metal phthalocyanines nanocomposite coatings for corrosion protection of carbon steel. J Mol Liq 220:513–517

25. Dagdag O, El Harfi A, Essamri A, El Gouri M, Chraibi S, Assouag M, et al (2018) Phosphorous-based epoxy resin composition as an effective anticorrosive coating for steel. Inter J Indus Chem. https://doi.org/10.1007/s40090-018-0152-5

26. Dagdag O, El Harfi A, Essamri A, El Bachiri A, Hajjaji N, Erramli. H, Hamed O, Jodeh S (2018) Anticorrosive performance of new epoxy-amine coatings based on zinc phosphate tetrahydrate

as a nontoxic pigment for carbon steel in NaCl medium. Arab J Sci Eng. https://doi.org/10.1007/s13369-018-3160-z

27. Ghaffari M, Ehsani M, Vandalvand M, Avazverdi E, Askari A, Goudarzi A (2015) Studying the effect of micro-and nano-sized ZnO particles on the curing kinetic of epoxy/polyaminoamide system. Prog Org Coat 89:277–283

28. Xu W, Wang Z, Han EH, Wang S, Liu Q (2018) Corrosion performance of Nano-ZrO_2 modified coatings in hot mixed acid solutions. Materials 11(6):934

29. Deflorian F, Rossi S, Fedel M, Motte C (2010) Electrochemical investigation of high-performance silane sol–gel films containing clay nanoparticles. Prog Org Coat 69(2):158–166

30. Montemor MF, Snihirova DV, Taryba MG, Lamaka SV, Kartsonakis IA, Balaskas AC, et al (2012) Evaluation of self-healing ability in protective coatings modified with combinations of layered double hydroxides and cerium molibdate nanocontainers filled with corrosion inhibitors. Electrochim Acta 60:31–40

31. Ammar S, Ramesh K, Vengadaesvaran B, Ramesh S, Arof AK (2016) Amelioration of anticorrosion and hydrophobic properties of epoxy/PDMS composite coatings containing nano ZnO particles. Prog Org Coat 92:54–65

32. Truc TA, Pébère N, Hang TTX, Hervaud Y, Boutevin B (2004) Evaluation of corrosion performance of a UV-cured polyurethane coating in the presence of organic phosphorous compounds. Prog Org Coat 49(2):130–136

33. Dagdag O, El Harfi A, El Gouri M, Touhami ME, Essamri A, Cherkaoui O (2016) Electrochemical impedance spectroscopy (SIE) evaluation of the effect of immersion time of the protective matrix based on a polymer tetra glycidyl of ethylene dianiline (TGEDA) on carbon steel in 3% NaCl. Inter J ChemTech Res 9(04):390–399

34. Ghasemi-Kahrizsangi A, Shariatpanahi H, Neshati J, Akbarinezhad E (2015) Corrosion behavior of modified nano carbon black/epoxy coating in accelerated conditions. Appl Surf Sci 331:115–126

35. Konios D, Stylianakis MM, Stratakis E, Kymakis E (2014) Dispersion behaviour of graphene oxide and reduced graphene oxide. J Col Interf Sci 430:108–112

36. Wu LK, Zhang JT, Hu JM, Zhang JQ (2012) Improved corrosion performance of electrophoretic coatings by silane addition. Corros Sci 56:58–66

37. Dagdag O, Hamed O, Erramli H, El Harfi A (2018) Anticorrosive performance approach combining an epoxy polyaminoamide-zinc phosphate coatings applied on sulfo-tartaric anodized aluminum alloy 5086. J Bio- Tribo-Corros 4(4):52

38. Alibakhshi E, Naeimi A, Ramezanzadeh M, Ramezanzadeh B, Mahdavian M (2018) A facile synthesis method of an effective anti-corrosion nanopigment based on zinc polyphosphate through microwaves assisted combustion method; comparing the influence of nanopigment and conventional zinc phosphate on the anti-corrosion properties of an epoxy coating. J Alloys Compd 762:730–744